

Supplemental Material for

# Thermodynamic Characterization of the Hydroxyls Group on the $\gamma$ -Alumina Surface by the Energy Distribution Function

*Matthieu Lagauche<sup>†</sup>, Kim Larmier<sup>†,§</sup>, Elsa Jolimaître<sup>\*†</sup>, Karin Barthelet<sup>†</sup>, Céline Chizallet<sup>†</sup>,  
Loïc Favergeon<sup>‡</sup>, Michèle Pijolat<sup>‡</sup>*

*<sup>†</sup> IFP Energies Nouvelles, Rond-Point de l'échangeur de Solaize, BP3, 69360 Solaize, France*

*<sup>‡</sup> Mines Saint-Etienne, LGF CNRS UMR5307, Centre SPIN, F-42023 St Etienne, France*

*<sup>§</sup> Department of Chemistry and Applied Biosciences, ETH Zürich, Vladimir-Prelog Weg 1-5,  
CH-8093, Zürich, Switzerland*

## S1. Characterization of the sample

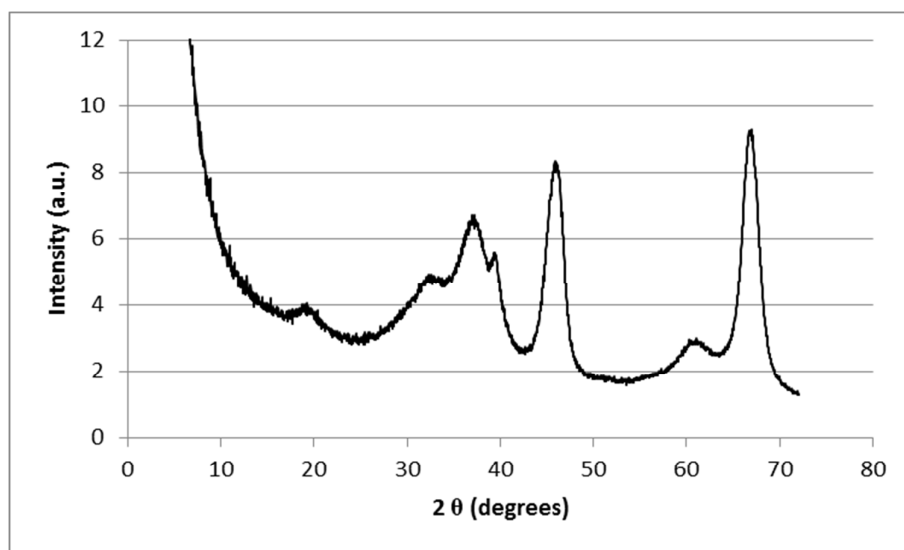


Figure S1.1: XRD pattern of the sample

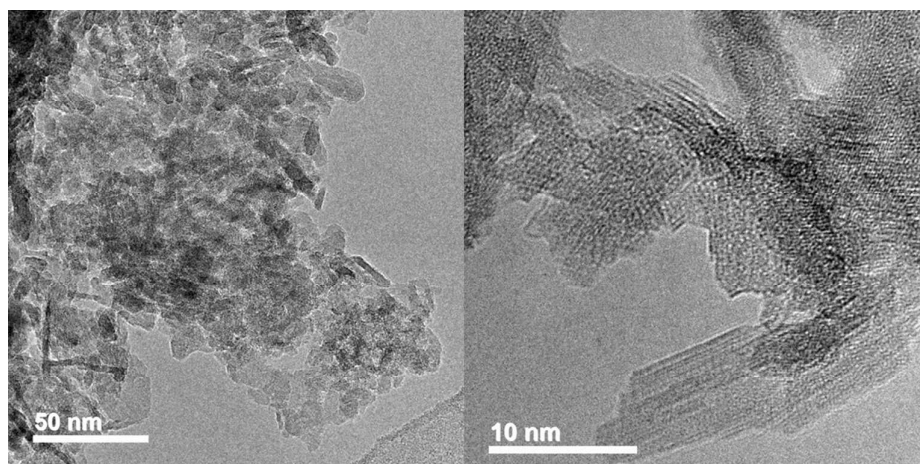
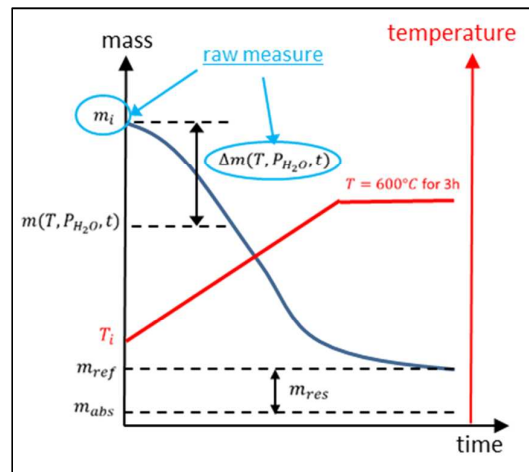


Figure S1.2: TEM pictures of the sample

## S2. Link between the relative and absolute hydroxyl coverage

The raw measurement in a TPD experiment are the initial mass  $m_i$  and the mass variation  $\Delta m$  as a function of time (see Figure S2.1). When the temperature is raised, the mass approaches the absolute mass of the alumina sample, but also the temperature of phase transition from  $\gamma$ - to  $\delta$ -alumina. The reference mass  $m_{ref}$  is therefore the one measured under the most dehydrating state obtainable with no risk of phase transition, i.e. 600°C (50°C under the temperature selected for the thermal decomposition of boehmite), 1 Pa of water (the lower partial pressure obtainable with our experimental device) and 3 h (time necessary to stabilize the mass signal).



**Figure S2.1:** Reference and absolute mass for TPD experiments.

The OH concentration on the surface with respect to the reference state is evaluated using the expression:

$$q^{\text{ref}}(T, P_{\text{H}_2\text{O}}, t) = \frac{m(T, P_{\text{H}_2\text{O}}, t) - m_{\text{ref}}}{m_{\text{ref}}} \quad \text{Eq. (S2.1)}$$

with:

$q^{\text{ref}}$ : the OH concentration with respect to the reference state (g g<sup>-1</sup>)

$m_{\text{ref}}$ : the mass at the reference state (g)

$m(T, P_{\text{H}_2\text{O}}, t)$ : the mass for a given operating condition (g)

Note that the absolute masses are calculated from the raw data using the following equation:

$$m = m_i - \Delta m \quad \text{Eq. (S2.2)}$$

To express the concentration in OH/nm<sup>2</sup>, the formula is:

$$q^{\text{ref}}(\text{OH nm}^{-2}) = q^{\text{ref}}(\text{g/g}) \frac{N_A \times 2}{M_{\text{H}_2\text{O}} \times S_{\text{BET}} \times 10^{18}} \quad \text{Eq. (S2.3)}$$

with:

$N_A$ : Avogadro number (mol<sup>-1</sup>)

$M_{\text{H}_2\text{O}}$ : molecular mass of water (g mol<sup>-1</sup>)

$S_{\text{BET}}$ : specific surface area of the sample (m<sup>2</sup> g<sup>-1</sup>)

To form a water molecule, two hydroxyls are needed, explaining the presence of a factor 2 at the numerator of eq. S2.3. In this paper, the experimental thermogravimetric data are compared with DFT simulations, which supply absolute OH concentrations. It is thus necessary to establish the relation between these two quantities.

The absolute surface OH concentration is:

$$q^{\text{abs}}(T, P_{\text{H}_2\text{O}}, t) = \frac{m(T, P_{\text{H}_2\text{O}}, t) - m_{\text{abs}}}{m_{\text{abs}}} \quad \text{Eq. (S2.4)}$$

with:

$$m_{\text{abs}} = m_{\text{ref}} - m_{\text{res}} \quad \text{Eq. (S2.5)}$$

where  $m_{\text{res}}$  is the mass corresponding to the residual hydroxyls present on the surface at the reference state (see Figure S2.1).

Expressing eq. S2.1 as a function of the absolute mass gives:

$$q^{\text{ref}}(T, P_{\text{H}_2\text{O}}, t) = \frac{m(T, P_{\text{H}_2\text{O}}, t) - m_{\text{abs}}}{m_{\text{abs}} + m_{\text{res}}} - \frac{m_{\text{res}}}{m_{\text{abs}} + m_{\text{res}}} \quad \text{Eq. (S2.6)}$$

If the mass of the residual hydroxyls is negligible compared to the mass of the dehydrated sample:

$$m_{\text{abs}} + m_{\text{res}} \approx m_{\text{abs}} \quad \text{Eq. (S2.7)}$$

we get:

$$q^{\text{abs}}(T, P_{\text{H}_2\text{O}}, t) = q^{\text{ref}}(T, P_{\text{H}_2\text{O}}, t) + q^{\text{res}} \quad \text{Eq. (S2.8)}$$

where  $q^{\text{res}}$  is the absolute residual surface concentration of OH groups:

$$q^{\text{res}} = \frac{m_{\text{res}} - m_{\text{abs}}}{m_{\text{abs}}} \quad \text{Eq. (S2.9)}$$

This means that the absolute concentration can be easily evaluated from the thermogravimetric data provided the residual OH concentration is known. In this paper, the residual OH concentration will be measured by chimimetry (see section 2.4. in the manuscript) and it will be shown that its mass is indeed negligible compared to that of the dehydrated sample.

From eq. S2.8, and knowing that the residual concentration is a constant, one can also write:

$$\frac{dq^{\text{abs}}(T, P_{\text{H}_2\text{O}}, t)}{dt} \approx \frac{dq^{\text{ref}}(T, P_{\text{H}_2\text{O}}, t)}{dt} \quad \text{Eq. (S2.10)}$$

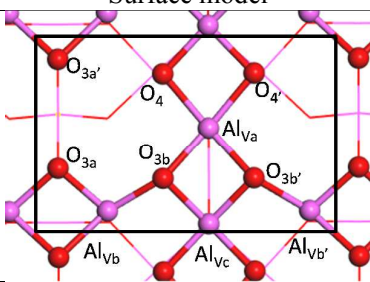
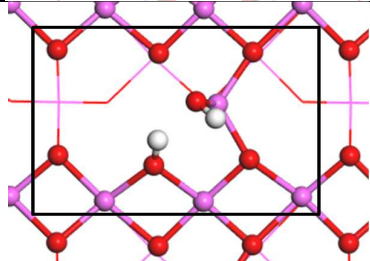
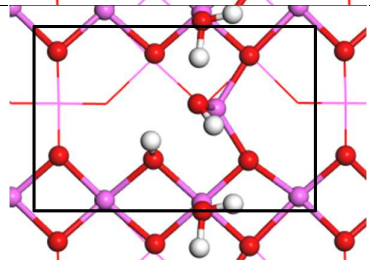
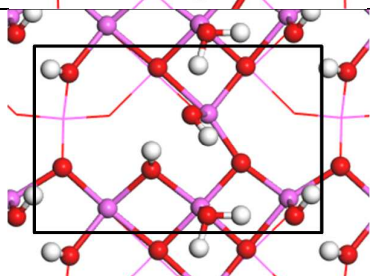
The desorption rates based on the absolute or the reference mass are hence equivalent. The energy distribution functions (EDF) can hence be directly estimated from the TPD data (without taking into account the residual hydroxyls).

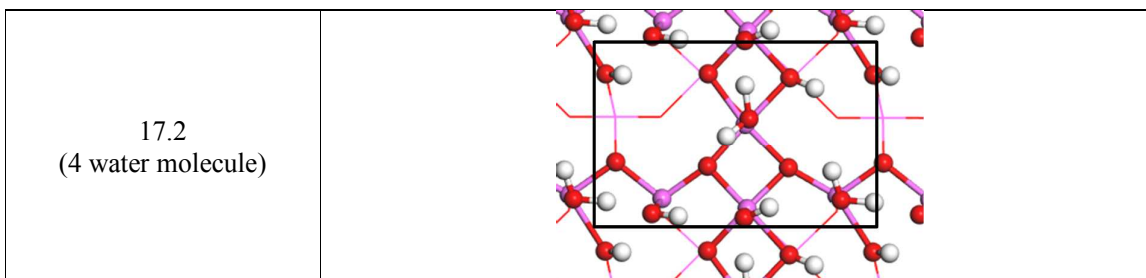
### **S3. Surface models considered in the DFT study**

**For all surface models depicted in the following, the color code is: red = oxygen, purple = aluminum, white = hydrogen.**

**(100) facets:**

The models used for the (100) facets are taken from Digne et al.<sup>1,2</sup> The structure were re-optimized at the PBE+D2 level without major changes, as reported earlier.<sup>3</sup>

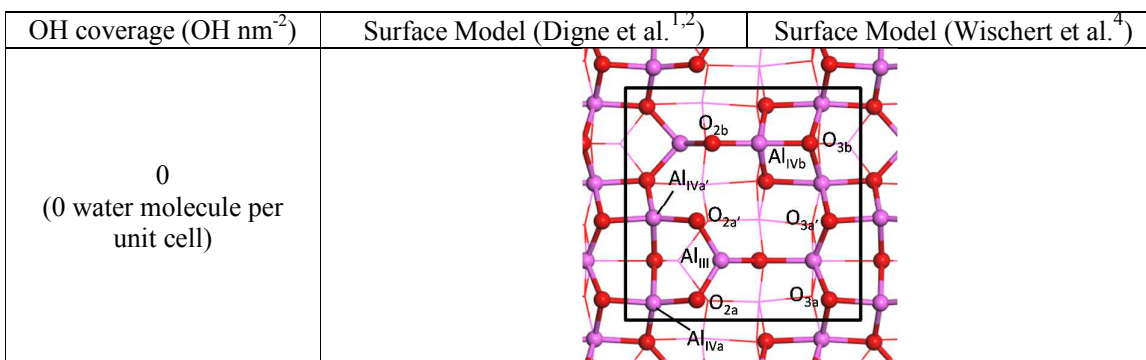
OH coverage (OH nm <sup>-2</sup> )	Surface model
0 (0 water molecule per unit cell)	
4.3 (1 water molecule)	
8.6 (2 water molecule)	
12.9 (3 water molecule)	

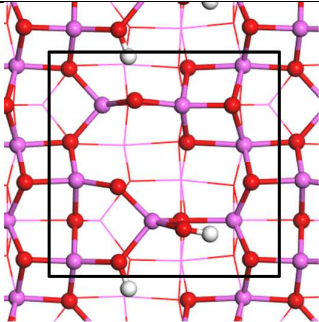
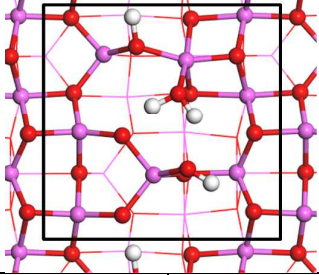
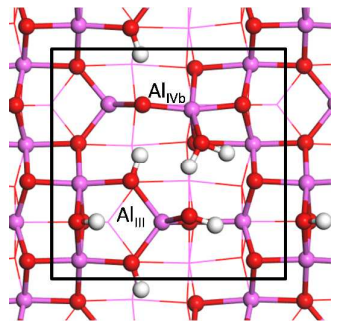
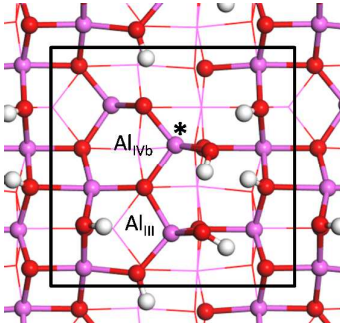
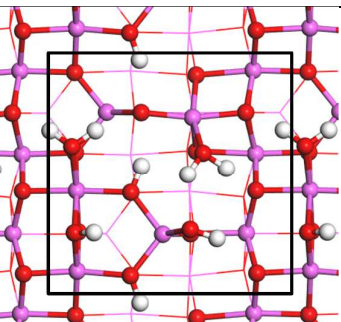
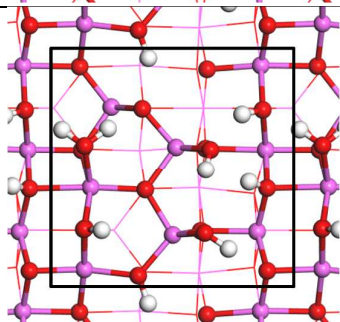
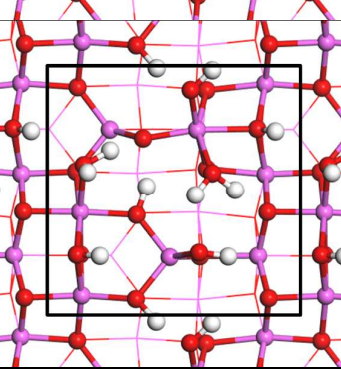
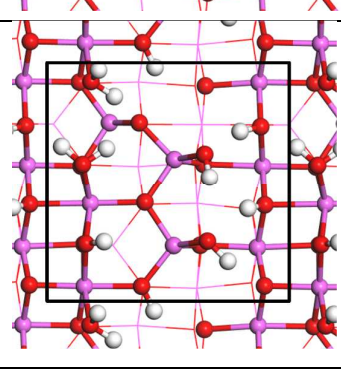


### **(110) facets:**

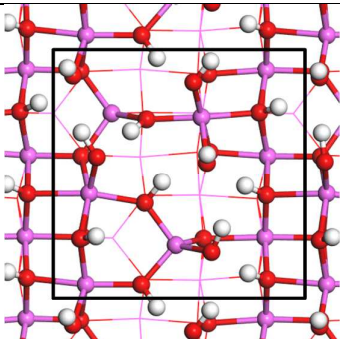
For the (110) facets, two different series of models were used. The first series originates from the models proposed by Digne et al.<sup>1,2</sup> Re-optimization at the PBE+D2 level only brings minor changes at the highest coverages (14.8 and 17.7 OH nm<sup>-2</sup>), as reported previously.<sup>3</sup> The second series originates from Wischert et al.<sup>4</sup> who proposed a surface reconstruction occurring from 8.9 OH nm<sup>-2</sup>. Namely, one of the aluminum atoms (Al<sub>Vb</sub> on the dehydrated surface) migrates into a tetrahedral position, as noted by a star on the corresponding model. This water induced reconstruction is thermodynamically favorable. The hydration further carries on from this reconstruction until the highest hydration state investigated (17.7 OH nm<sup>-2</sup>), where the aluminum atoms moves back to its original position.

Overall, the 2 series of models are identical for several coverages (0, 3.0, 5.9 and 17.7 OH nm<sup>-2</sup>) but differ for 8.9, 11.8 and 14.8 OH nm<sup>-2</sup>.



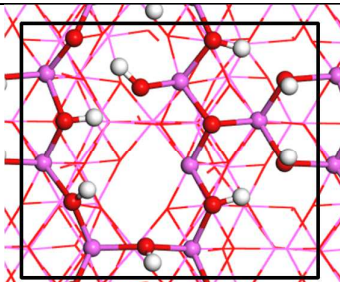
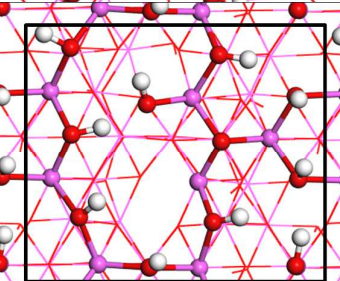
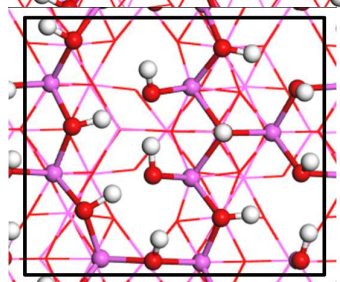
<p>3.0 (1 water molecule)</p>		
<p>5.9 (2 water molecule)</p>		
<p>8.9 (3 water molecule)</p>		
<p>11.8 (4 water molecule)</p>		
<p>14.8 (5 water molecule)</p>		



17.7 (6 water molecule)	
----------------------------	--

### **(111) facets**

The (111) surface models employed are inspired from ref.1,2. The structures were re-optimized at the PBE+D2 level without major changes.

OH coverage ( $\text{OH nm}^{-2}$ )	Surface model
9.8 (4 water molecule per unit cell)	
12.3 (5 water molecule)	
14.7 (6 water molecule)	

## S4. Adsorption features calculated by DFT

**Table S4.1.**  $\Delta_{\text{ads}}H$  and  $\Delta_{\text{ads}}S$  from DFT calculations for the successive hydration reactions leading to the given surface coverage, taking place at the (110) alumina surface, according to models inspired from Digne et al.<sup>1,2</sup>

$q_{i,(110)} \text{ (OH /nm}^{-2}\text{)}$	3.0	5.9	8.9	11.8	14.8	17.7
$\Delta_{\text{ads}}H \text{ (kJ mol}^{-1}\text{)}$	-236	-198	-147	-127	-99	-110
$\Delta_{\text{ads}}S \text{ (J mol}^{-1} \text{ K}^{-1}\text{)}$	-186	-186	-160	-175	-186	-186

**Table S4.2.**  $\Delta_{\text{ads}}H$  and  $\Delta_{\text{ads}}S$  from DFT calculations for the successive hydration reactions leading to the given surface coverage, taking place at the (110) alumina surface, according to models inspired from Wischert et al.<sup>4</sup>

$q_{i,(110)} \text{ (OH nm}^{-2}\text{)}$	3.0	5.9	8.9	11.8	14.8	17.7
$\Delta_{\text{ads}}H \text{ (kJ mol}^{-1}\text{)}$	-228	-196	-167	-135	-69	-54
$\Delta_{\text{ads}}S \text{ (J mol}^{-1} \text{ K}^{-1}\text{)}$	-148	-186	-158	-165	-167	-163

**Table S4.3.**  $\Delta_{\text{ads}}H$  and  $\Delta_{\text{ads}}S$  from DFT calculations for the successive hydration reactions leading to the given surface coverage, taking place at the (100) alumina surface.

$q_{i,(100)} \text{ (OH nm}^{-2}\text{)}$	4.3	8.6	12.9	17.2
$\Delta_{\text{ads}}H \text{ (kJ mol}^{-1}\text{)}$	-100	-110	-89	-60
$\Delta_{\text{ads}}S \text{ (J mol}^{-1} \text{ K}^{-1}\text{)}$	-157	-169	-176	-143

**Table S4.4.**  $\Delta_{\text{ads}}H$  and  $\Delta_{\text{ads}}S$  from DFT calculations for the successive hydration reactions leading to the given surface coverage, taking place at the (111) alumina surface.

$q_{i,(111)} \text{ (OH/nm}^{-2}\text{)}$	12.3	14.7
$\Delta_{\text{ads}}H \text{ (kJ mol}^{-1}\text{)}$	-234	-160
$\Delta_{\text{ads}}S \text{ (J mol}^{-1} \text{ K}^{-1}\text{)}$	-161	-197

**S5. EDF obtained from DFT data, with the alumina model inspired from Wischert et al.**

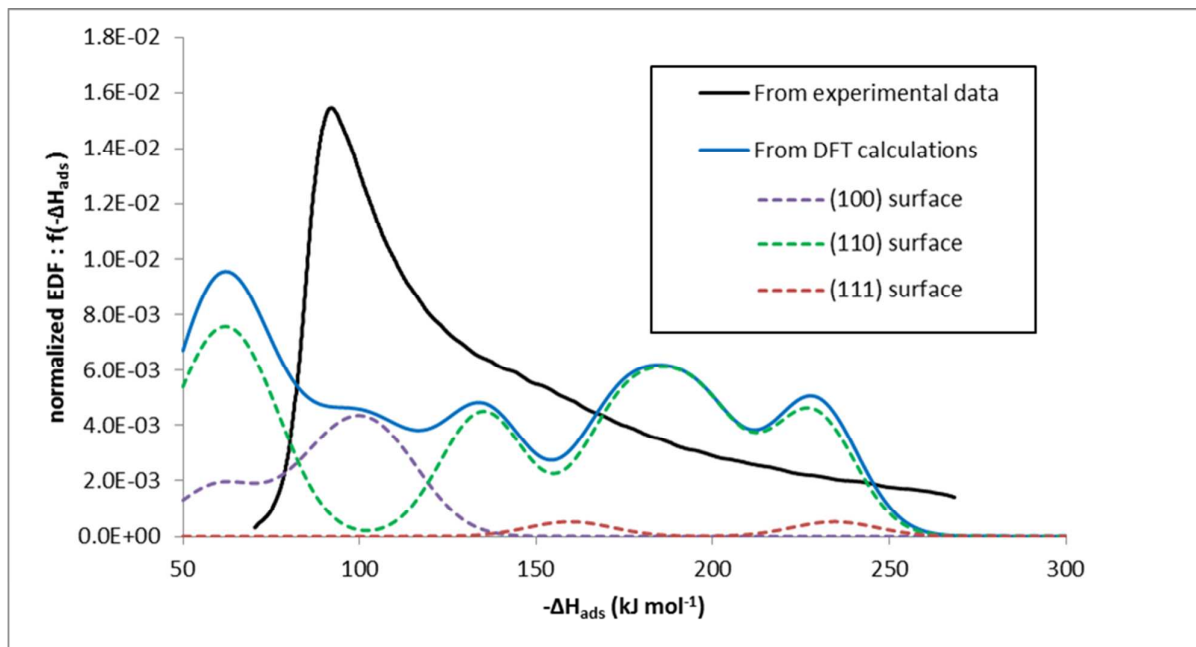


**Figure S5.1.** Energy Distribution Function (EDF) of the sample, obtained from experimental and DFT data, with models inspired from Wischert et al.<sup>4</sup> for the (110) surface. In the latter case, the individual contributions from the three main crystallographic surfaces is shown.

**S6. Adsorption isotherms obtained from DFT calculations, with the alumina model inspired from Wischert et al.**

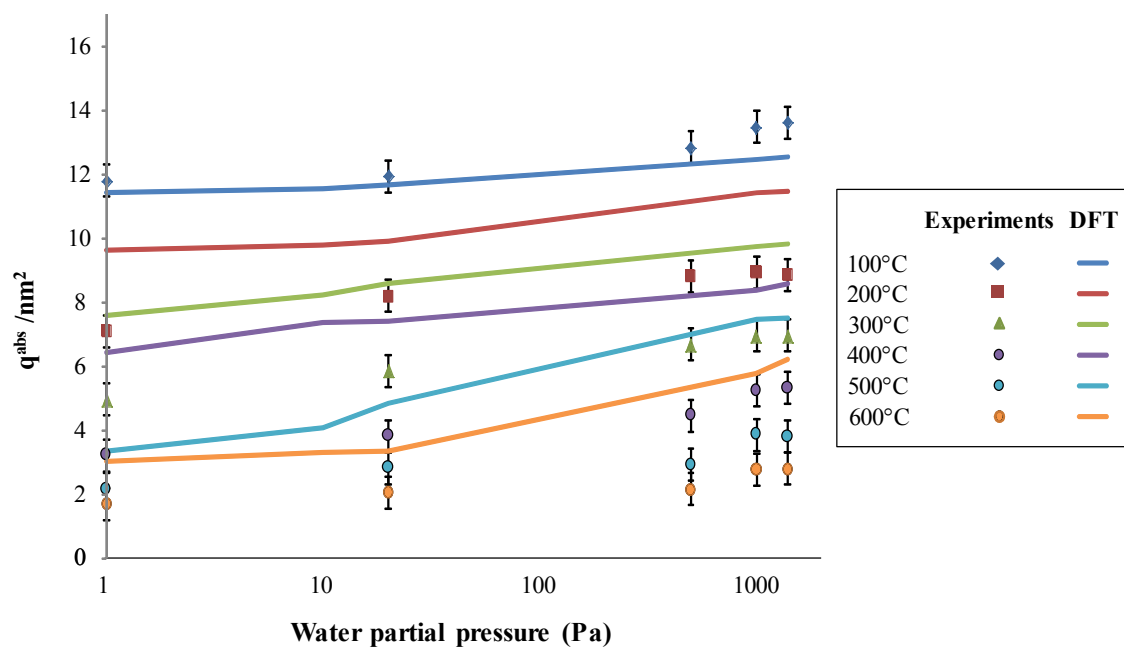


**Figure S6.1.** Comparison between experimental adsorption isotherms and DFT calculations (Wischert et al. model).

## References

- 1 Digne, M.; Sautet, P.; Raybaud, P.; Euzen, P.; Toulhoat, H. Hydroxyl Groups on  $\gamma$ -Alumina Surfaces: A DFT Study. *J. Catal.* **2002**, *211*, 1-5.
- 2 Digne, M.; Sautet, P.; Raybaud, P.; Euzen, P.; Toulhoat, H. Use of DFT to Achieve a Rational Understanding of Acid–Basic Properties of  $\gamma$ -Alumina Surfaces. *J. Catal.* **2004**, *226*, 54-68.
- 3 Larmier, K.; Chizallet, C.; Cadran, N.; Maury, S.; Abboud, J.; Lamic-Humblot, A.-F.; Marceau, E.; Lauron-Pernot, H. Mechanistic Investigation of Isopropanol Conversion on Alumina Catalysts: Location of Active Sites for Alkene/Ether Production. *ACS Catalysis* **2015**, *5*, 4423-4437.
- 4 Wischert, R.; Laurent, P.; Copéret, C.; Delbecq, F.; Sautet, P.  $\gamma$ -Alumina: The Essential and Unexpected Role of Water for the Structure, Stability, and Reactivity of "Defect" Sites. *J. Am. Chem. Soc.* **2012**, *134*, 14430-14449.